Toward selective anticancer metallodrugs

Rixel, V.H.S. van; Rixel V.H.S. van

CHAPTER 3

A microtubule-targeted rigidin analogue caged by a ruthenium polypyridyl complex that can be released with green light

This chapter is to be submitted as a full paper: Vincent H.S. van Rixel, Tugba Ozel, Tania Betancourt, Lucien N. Lameijer, Alexander Kornienko, Sylvestre Bonnet, *manuscript in preparation*.

3.1 Introduction

Microtubules play an essential role in mitosis, specifically in the separation of duplicated chromosomes before the cell divides.[1] This feature makes them a potential target for novel chemotherapeutic agents. Paclitaxel, a taxane drug used in clinics to treat various forms of breast, ovarian, and non-small cell lung cancer, promotes polymerization of stable and dysfunctional microtubules that in the end causes cell death.[2] However, side effects associated with the use of paclitaxel are not uncommon, and include neutropenia, neurotoxicity, and disturbances in cardiac rhythm.[3, 4] Additionally, cancer cell resistance to paclitaxel therapy limits its clinical efficacy making the development of alternative microtubule-targeting agents an important area of research.

One family of alternative compounds are analogues derived from marine alkaloid rigidins.[5, 6] These rigidins have shown cytotoxic activity in the low-nanomolar range, trigger complete collapse of mitotic microtubule organization *in vitro*, and result in significant tumor growth reduction *in vivo*. However, drug uptake by healthy tissues causing side effects can always jeopardize the success of a drug. In this work we investigated the functionalization of the original 7-deaxahypoxanthines with a thioether group at the C2-position, and coordination of this thioether to a light-activatable ruthenium complex, a strategy called 'photocaging'.[7-15] Upon light irradiation, the metal complex undergoes a photosubstitution reaction in which the ligand is released and can interact with its biological target. Photocaging is part of the phototherapeutic approach of photoactivated chemotherapy (PACT), a concept in which a metal complex is prevented from interaction with biological molecules in the dark.[13] After light activation the metal complex is structurally modified, commonly through the release of a ligand, and then either the free ligand or complex (or both) may bind to their targets. Overall, the photochemical local activation of anticancer prodrugs in cancerous tissue should limit the toxicity of the treatment to the irradiated tumor, thus lowering side effects that stem from the general toxicity of biologically active compounds.

Ruthenium(II) polypyridyl complexes belong to the most widely investigated PACT compounds due to their well-known and tunable light absorption properties. For example, irradiation of RuBiGABA-2 (see Figure 3.1) developed by

Etchenique releases γ-aminobutyric acid, which was shown to induce a motoneural response in leech ganglions.[16] In another example from Turro the nitrile analogue 5CNU of clinically approved anticancer compound 5-fluorouracil was caged with ruthenium, triggering to form $[Ru(tpy)(5\text{-}CNU)_3]Cl_2$ (Figure 3.1) phototoxicity in HeLa cells as demonstrated by a qualitative SYTOX assay.[7] Recently, our group reported toxic ruthenium polypyridyl complexes that photosubstitute sulfoxide or thioether ligands upon blue or green light activation, and induce a phototoxic response in human cancer cell lines.[17-19] In this chapter the successful caging of the thioether-containing rigidin 7-deazahypoxanthines **1** (provided by Dr. Alexander Kornienko) by a $[Ru(tpy)(bpy)]^{2+}$ moiety that can be released upon green light irradiation is reported. To the best of our knowledge, this is the first example of an anticancer drug with a well-defined target, which is caged by a ruthenium complex. Quantitative *in vitro* data on cancer cell cytotoxicity in the dark and after light irradiation is provided, including strong evidence that confirms the light-controllable the interaction of our drug with the microtubules.

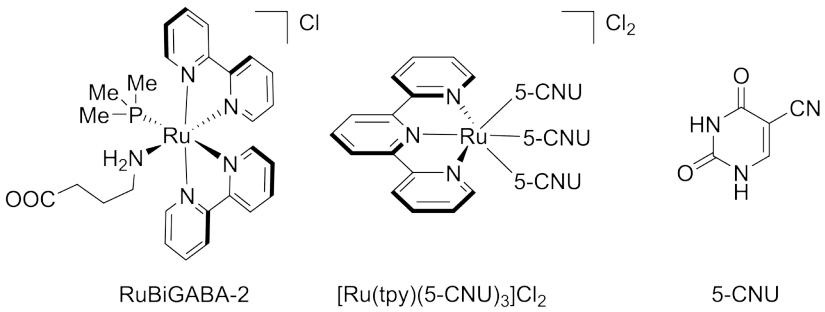

Figure 3.1 Chemical structures of RuBiGABA-2, $[Ru(tpy)(5\text{-}CNU)_3]Cl_2$, and 5-CNU.

3.2 Results

3.2.1 Synthesis

Complex $[Ru(tpy)(bpy)(\mathbf{1})](PF_6)_2$ ($[\mathbf{2}](PF_6)_2$) was synthesized by reacting **1** with 2 equivalents of $[Ru(tpy)(bpy)(OH_2)](PF_6)_2$ ($[\mathbf{3}](PF_6)_2$) as shown in Scheme 3.1. ^1H NMR spectroscopy showed the characteristic upfield shift at 1.47 ppm of the coordinated SMe group, that is normally found around > 2.0 ppm in protic solvents

for these type of complexes. Comparison with the free ligand is lacking due to its poor solubility in protic solvents.[20] Further NMR spectroscopy and elemental analysis showed that the compound was pure, and high resolution mass spectrometry confirmed the successful synthesis of [**2**](PF$_6$)$_2$.

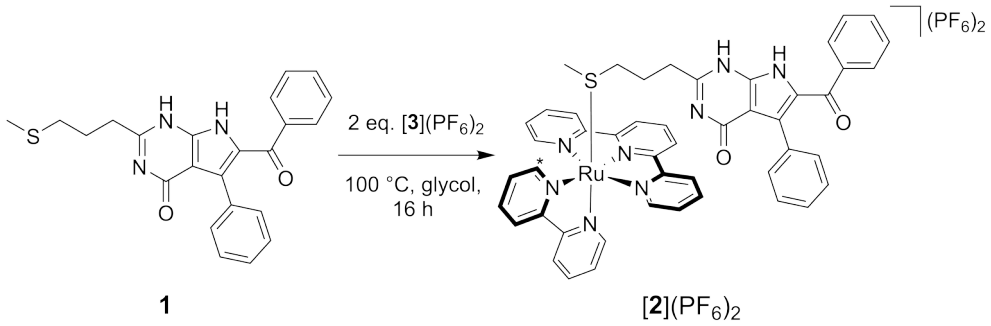

1 [**2**](PF$_6$)$_2$

Scheme 3.1 Synthesis scheme of [2](PF$_6$)$_2$. * indicates the A6 proton of the bpy ligand.

3.2.2 Photochemistry

Under green light irradiation (λ_{irr} = 530 nm) of a solution of [**2**](PF$_6$)$_2$ in acetonitrile in a nitrogen atmosphere, a significant increase of the absorbance at 452 nm and a slight shift of the maximum of the ^{1}MLCT band from 452 nm to 454 nm were observed (Figure 3.2). Under these conditions a steady state was obtained after 30 minutes (inset in Figure 3.2). Mass spectrometry (MS) of the solution after light irradiation showed peaks at m/z = 266.4 corresponding to [Ru(tpy)(bpy)(CH$_3$CN)]$^{2+}$ (calc. m/z = 266.1, Figure SIII.1), whereas MS of the dark control showed a major signal at m/z = 447.0 corresponding to [**2**]$^{2+}$ (calc. m/z = 447.1, Figure SIII.1). Thus, under irradiation ligand **1** was photosubstituted by a solvent molecule. Similar evolutions were observed under blue light irradiation (450 nm, Figure SIII.2) and under such conditions a photosubstitution quantum yield Φ_{PS} of 0.0060 was obtained. The photoreaction was also monitored by ^{1}H NMR. After 5 minutes irradiation by white light the characteristic A6 proton (Scheme 3.1) at 9.66 ppm from the bpy ligand was fully replaced by a peak at 9.59 ppm characteristic for [Ru(tpy)(bpy)(CH$_3$CN)]$^{2+}$, indicating full conversion of the photoreaction of [**2**]$^{2+}$ (Figure SIII.3).[21] Also, the initial singlet peak at 1.32 ppm indicating coordinated SMe is fully replaced by a singlet peak at 2.54 ppm for non-coordinated **1**. When the same light irradiation reaction was performed in demineralized water and followed by UV-vis spectroscopy, Rayleigh scattering occurred quickly due to

precipitation of the free ligand **1**, which is poorly soluble in water with a maximum solubility of 10 μM in demineralized water (Figure SIII.4). Thus, it can be concluded that the Ru-S bond of $[\mathbf{2}]^{2+}$ is photoactivatable in CH_3CN and aqueous solution using either blue, green, or white light.

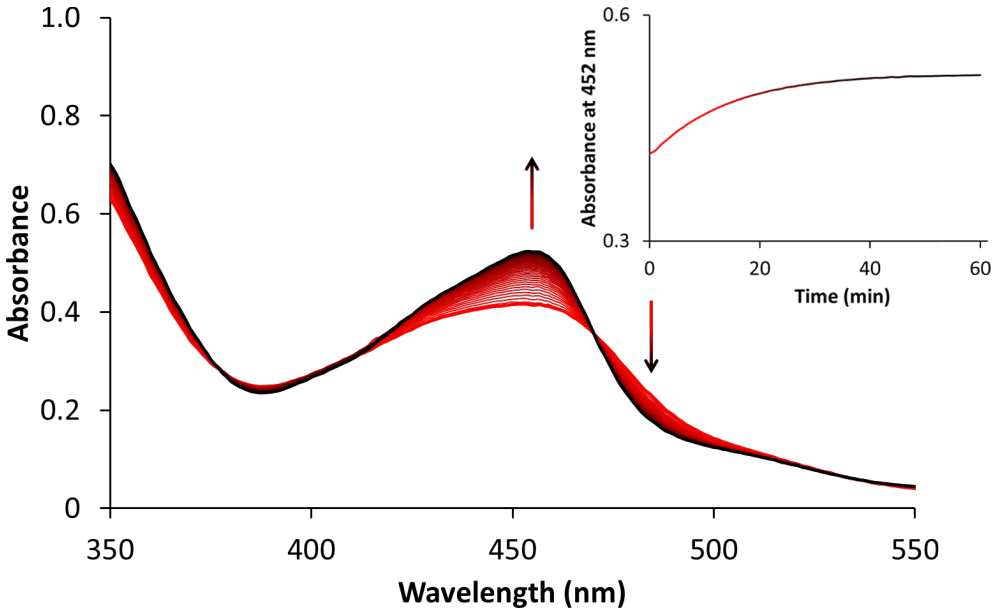

Figure 3.2 Evolution of the electronic absorption spectra of a solution of $[\mathbf{2}](PF_6)_2$ in acetonitrile upon green light irradiation under nitrogen (λ = 530 nm, $\Delta\lambda_{1/2}$ = 17 nm, 6.0 mW, photon flux 4.1× 10^{-8} mol.s^{-1}). Time: 0 min (red curve) to 30 min (black curve) Conditions: $[Ru]_0$ = 50 μM, V = 3.00 mL, T = 293 K. Inset: Plot of the absorbance at 452 nm as a function of irradiation time.

3.2.3 (Photo)toxicity studies

To demonstrate whether cytotoxicity of $[\mathbf{2}](PF_6)_2$ could be controlled by light activation, an *in vitro* photocytotoxicity assay was performed. The cytotoxicity of **1**, $[\mathbf{2}](PF_6)_2$, and $[\mathbf{3}](PF_6)_2$ was investigated against cancerous A375, A431, and A549 cells, and non-cancerous MRC-5 cells. $[\mathbf{3}](PF_6)_2$ was included in the assay to ensure that cytotoxicity does not originate from the metal cage, while cisplatin was included as positive control. Cell growth inhibition effective concentrations (EC_{50}), defined as the compound concentration that reduces cell viability by 50% compared to untreated cells, were measured in the dark and after light activation

following a protocol adapted from Hopkins et al.[22] and the results are reported in Table 3.1. In the dark EC_{50} values between 0.16 μM and 0.23 μM were found for **1** in A375, A431, and MRC-5 cells, and a higher value of 6.5 μM was found for A549 cells. Compound [**3**]$(PF_6)_2$ showed no activity across all tested cell lines, which is in agreement with previous findings,[19] while treatment with cisplatin resulted in EC_{50} values in the expected micromolar range, i.e. between 0.85-3.1 μM. For the caged compound [**2**]$(PF_6)_2$ in the dark, EC_{50} values of 7-14 μM in A375, A431, and MRC-5 cells were observed, while for A549 cells an EC_{50} value of 35 μM was measured. Thus, caging of **1** to the $[Ru(tpy)(bpy)]^{2+}$ moiety strongly inhibited, up to 83 times for MRC-5 cells, the cytotoxicity of the microtubule inhibitor in the dark.

Table 3.1 Cell growing inhibition effective concentrations (EC_{50} values with 95% confidence interval in μM) of 1, [2]$(PF_6)_2$, [3]$(PF_6)_2$, and cisplatin on skin (A375, A431) and lung (A549) cancer cell lines. The photo index (PI), defined as $EC_{50,dark}/EC_{50,light}$, are also indicated. Toxicity of the compounds in non-cancerous lung cell line (MRC-5) were also tested for comparison.

		1		**[2]$(PF_6)_2$**			**[3]$(PF_6)_2$**	**cisplatin**	
Cell Line	**Light dose ($J.cm^{-2}$)**	**EC_{50} (μM)**	**±CI**	**EC_{50} (μM)**	**±CI**	**P.I**	**EC_{50} (μM)**	**EC_{50} (μM)**	**±CI**
A375	0	0.16	–0.053 +0.079	6.8	–1.4 +1.7	21	> 100	0.85	–0.079 +0.087
	38	0.20	–0.069 +0.11	0.33	–0.11 +0.16		> 100	0.87	–0.062 +0.067
A431	0	0.23	–0.028 +0.032	14	–3.0 +3.9	28	> 100	2.8	–0.28 +0.31
	38	0.24	–0.038 +0.045	0.49	–0.059 +0.067		> 100	3.1	–0.37 +0.43
A549	0	6.5	–1.5 +2.0	35	–8.7 +12	4	> 100	1.3	–0.41 +0.62
	38	3.4	–0.47 +0.54	9.2	–4.0 +7.1		> 100	2.0	–0.30 +0.36
MRC-5	0	0.17	–0.07 +0.13	8.1	–1.4 +1.7	9	> 100	1.5	–0.20 +0.23
	38	0.34	–0.15 +0.27	0.67	–0.28 +0.49		> 100	2.2	–0.23 +0.26

Green light (520 nm) was chosen for photochemical activation since *in vitro* and *in vivo* it is much less toxic to living cells than blue or UV-light.[22-24] Preliminary studies in a 96-well plate (Figure SIII.5) demonstrated that under the conditions of our cell-irradiation setup (21 mW.cm^{-2}) a 30 minutes irradiation time, corresponding to a dose of 38 J.cm^{-2}, was necessary to completely activate [**2**](PF$_6$)$_2$ (60 μM). Although a 38 J.cm^{-2} dose of green light barely induced photocytotoxicity by itself, nor changed the cytotoxicity of the uncaged inhibitor **1**, the caging complex [**3**](PF$_6$)$_2$, or cisplatin (Table 3.1), the effect observed when the caged inhibitor [**2**](PF$_6$)$_2$ was irradiated was remarkable for all cell lines tested. EC$_{50}$ values for A375, A431, A549, and MRC-5 cells were 0.33, 0.49, 9.2, and 0.67 μM, leading to phototoxic indices of 21, 28, 4, and 12, respectively. Figure 3.3 shows, as an example, the dose-response curves for A431 cells treated with **1** (brown curve), [**2**](PF$_6$)$_2$ in the dark (black curve), [**2**](PF$_6$)$_2$ irradiated with green light (green curve), and [**3**](PF$_6$)$_2$ in the dark (grey curve). The data suggests that [Ru(tpy)(bpy)]$^{2+}$ is an excellent photocaging agent for **1** as Ru-coordination strongly reduces the cytotoxicity of **1**, while photosubstitution performed in living cells restores a high toxicity typical for ligand **1**.

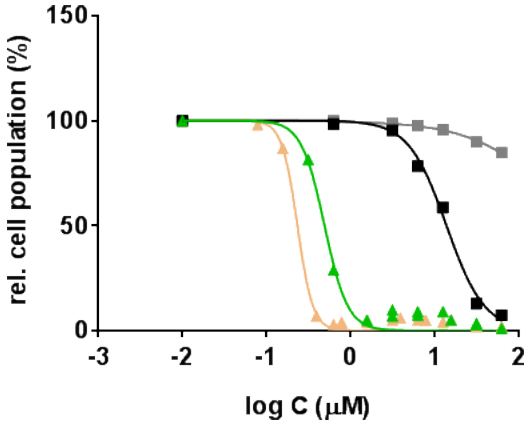

Figure 3.3 Dose response curves for A431 cells incubated with 1 in the dark (light brown), [2](PF$_6$)$_2$ in the dark (black), [2](PF$_6$)$_2$ with green light irradiation (green), and [3](PF$_6$)$_2$ in the dark (grey). Phototoxicity assay: cells seeded at 8 × 10^3 cells/well at t = 0 h, treated at t = 24 h, irradiated at t = 30 h, and SRB assay performed at t = 96 h. Conditions: T = 37 °C, v/v% CO_2 = 7%, λ_{irr} = 520 nm, light dose = 38 J.cm^{-2}.

3.2.4 Tubulin polymerization assay

In order to investigate how caging and photoactivation influences the ability of compound [**2**]$(PF_6)_2$ to interact with its biological microtubule target, a fluorescence-based tubulin polymerization assay was performed by Dr. Tania Betancourt to compare the tubulin polymerization properties of [**2**]$(PF_6)_2$ in the dark and under light irradiation. In this assay tubulin polymerization leads to a marked increase of the fluorescence intensity. The control compound paclitaxel, which strongly stabilizes the polymerized microtubule, showed as expected a rapid rise in fluorescence that stabilized after 30 minutes, indicating nucleation, growth, and a steady state equilibrium, of the microtubule formulation as shown in Figure 3.4.[5] Fluorescence of an untreated sample initially shows a slight reduction in intensity and then stabilizes around its original value as shown by the dashed curve in Figure 3.4. Treatment of the tubulin mixture with the caged inhibitor [**2**]$(PF_6)_2$ (25 μM, black curve) showed, in the dark, an overall increase in fluorescence after 60 minutes which was slower and less prominent than that measured for paclitaxel. Treatment with the caged inhibitor [**2**]$(PF_6)_2$ (25 μM) activated by green light irradiation (30 min, 21 $mW.cm^{-2}$) showed no increase in fluorescence at all. These results demonstrate that indeed upon treatment with non-activated [**2**]$(PF_6)_2$ tubulin polymerization is possible, i.e., the caged inhibitor does not inhibit polymerization, whereas after green light activation of [**2**]$(PF_6)_2$ tubulin polymerization is inhibited. In other words, green light irradiation uncages the inhibitor **1** efficiently. To conclude, microtubule polymerization is controlled by light. Green light activation of [**2**]$(PF_6)_2$ inhibits microtubule polymerization by release of **1**.

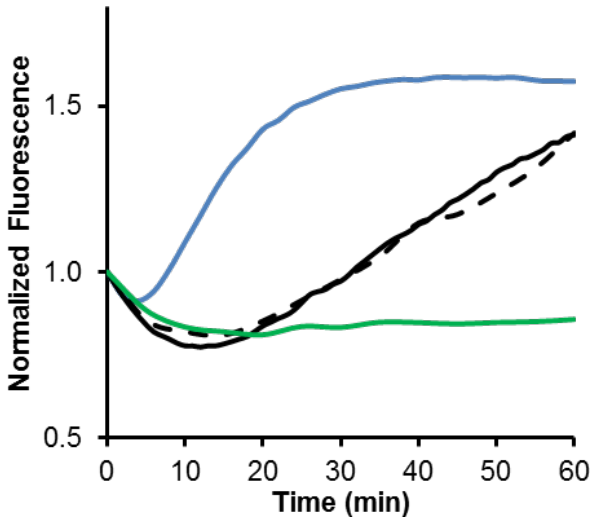

Figure 3.4 Evolution of tubulin polymerization [2](PF$_6$)$_2$ in the dark (25 μM, black curve), green light-activated [2](PF$_6$)$_2$ (25 μM, green curve), Paclitaxel (3 μM, blue curve), and untreated sample (black dashed curve).

3.3 Discussion & Conclusion

In this chapter we have demonstrated that the microtubulin-targeted rigidin thioether conjugate **1** can be caged by [Ru(tpy)(bpy)]$^{2+}$. *In vitro* green light photosubstitution of the ruthenium-caged rigidin in [**2**](PF$_6$)$_2$ induces an up to 28-fold increase in cytotoxicity with values that are similar to that of the uncaged compound **1**. As many microtubule-targeting compounds are used in the clinic as anticancer compounds,[1, 25, 26] the herein presented strategy of ruthenium caging and green light photorelease provides a basis for a new cancer-targeted photoactivated chemotherapy. This strategy is clearly distinct from the approach of organic chemists in photopharmacology, where azobenzene-functionalized protein inhibitors are switched 'on' and 'off' via *cis-trans* photoizomerization.[27-30] Coordination of an inhibitor to a light-sensitive metal complex, as proposed in this work, can overcome several issues associated with the azobenzene isomerization approach. First, in photopharmacology the light activation wavelength is crucial. Low-energy green or red light can penetrate into tissues much deeper, and is less harmful, than high-energy UV or blue light. Although recently some azobenzenes have been developed that can be activated by visible or even red light,[31-33] ruthenium polypyridyl chemistry provides a solid, tunable, and predictive fundament for making photopharmacological agents that can be activated by

visible light.[13, 34-37] Second, as azobenzenes have a low or no dipole moment, especially in their *trans* form, they are highly lipophilic and poorly water-soluble. Ruthenium complexes on the other hand are typically positively charged molecules, which can enhance water solubility. Next, contrary to azobenzenes the modification of the cage does not alter too much the photoactivation kinetics. Last but not least, light activation of metal-based PACT compounds usually entails an irreversible process, whereas *cis-trans* photoisomerization of azobenzenes is notoriously reversible. Permanent activation of azobenzene-functionalized compounds would require permanent irradiation to maintain activity. On the other hand, it may provide opportunities for limiting systemic toxicity to the activated area, as when not irradiated the compound turns back into a non-toxic form. With metal caging, irreversible activation at the place of irradiation may be followed by diffusion of the activated drugs in other places, which for *in vivo* applications, would need to be controlled.

In the development of anticancer drugs both organic and inorganic chemists cope with similar problems, i.e. drug resistance, dose-limiting side effects, and poor water solubility. In this chapter the use of combining organic chemistry, which offers stable compounds and well-defined targets, with inorganic caging compounds, which can reduce dark toxicity, increase water solubility, and allow for irreversible uncaging using visible light, demonstrates how both fields are complementary. By crossing research borders, innovative solutions can be found that can contribute to ground-breaking developments in photopharmacology and science.

3.4 Experimental

3.4.1 Materials and methods

All NMR spectra were recorded on a Bruker AV-500 spectrometer. Chemical shifts are indicated in ppm relative to tetramethylsilane. Mass spectra were recorded by using a MSQ Plus Spectrometer positive ionization mode. UV-vis experiments were performed on a Cary 50 Varian spectrometer equipped with a Cary Single Cell Peltier for temperature control.

3.4.2 Synthesis of [Ru(tpy)(bpy)(1)](PF$_6$)$_2$ ([2](PF$_6$)$_2$)

First, **1** and [**3**](PF$_6$)$_2$ were synthesized according to literature procedures.[5, 21] Then, in a 2-necked round-bottom flask [**3**](PF$_6$)$_2$ (75 mg, 0.48 mmol) and **1** (22 mg, 0.25 mmol) were added in ethylene glycol (10 mL) under argon. The solution was stirred overnight at 100 °C

under argon resulting in a red solution. The reaction mixture was added to a CH_2Cl_2 and KPF_6 saturated water mixture. After full extraction to the CH_2Cl_2 layer, the combined CH_2Cl_2 layers were washed with KPF_6 saturated water to remove ethylene glycol. After evaporation *in vacuo*, the crude was dissolved in acetone and purified by size exclusion chromatography (Sephadex LH-20, acetone). After evaporation *in vacuo*, the product was reprecipitated from acetone by the addition of diethyl ether, filtered, and obtained as a red powder. Yield: 13 mg (20%). *^{1}H NMR (500 MHz, CD_3OD, 293 K, in ppm)*: δ = 9.74 (d, *J* = 5.5 Hz, 1H, A6), 8.82 (d, *J* = 8.0 Hz, 1H, A3), 8.72 (d, *J* = 8.0 Hz, 2H, D3 + D3'), 8.69 (d, *J* = 8.0 Hz, 1H, B3), 8.51 (t, *J* = 8.0 Hz, 2H, C3 + C3'), 8.39 (dd, *J* = 8.0, 1.2 Hz, 1H, A4), 8.37 (dd, *J* = 8.4, 1H, D4), 8.03 (ddd, *J* = 7.8 Hz, 5.5 Hz, 1.5 Hz, 1H, A5), 7.95 (dd, *J* = 8.0 Hz, 2H, C4 + C4'), 7.92 (dd, *J* = 7.5 Hz, 1.5 Hz), 1H, B4), 7.73 (d, *J* = 5.5 Hz, 2H, C6), 7.52 (dd, *J* = 8.5, 1.0 Hz, 2H, Ph), 7.35 (ddd, *J* = 0.5, 6.0, 6.0 Hz, 2H, C5), 7.32-7.18 (m, 5H, Ph + B5), 7.14-7.05 (m, 5H, Ph + B6), 2.63 (t, *J* = 6Hz, 2H, CH_2), 1.91 (p, *J* = 7.0 Hz, 2H, CH_2), 1.91 (t, *J* = 7.5 Hz, 2H, CH_2), 1.47 (s, 3H, CH_3). *^{13}C NMR (125 MHz, CD_3OD, 293 K, in ppm)*: δ = 190.4 (C=O), 161.7 (pp), 159.2 (pp), 158.8 (pp), 158.7 (pp), 158.1 (pp), 158.1 (pp), 154.2 (Ph), 153.0 (Ph), 151.2 (Ph), 150.8 (Ph), 140.1 (Ph), 139.6 (C4), 138.6 (py-q), 138.3 (D4), 133.7 (py-q), 133.3 (A6), 132.6 (Ar), 130.6 (Ar), 129.7 (Ar-q), 129.4 (Ar-q), 129.2 (A5), 129.1 (C5), 128.9 (Ar), 126.1 (C3'), 126.0 (C3), 125.4 (A3), 125.2 (D3), 32.8 ($CH_{2\text{-}r}$), 32.80 ($CH_{2\text{-}l}$), 23.7 (CH_2), 14.6 (CH_3). *Elem. Anal. Calcd. for $C_{48}H_{40}F_{12}N_8O_2P_2RuS$*: C, 48.69; H, 3.41; N, 9.46. Found: C, 49.35; H, 3.53; N, 9.32. *High resolution ES MS m/z (calc)*: 447.10198 (447.1019, $[M - 2\times PF_6]^{2+}$).

3.4.3 Photochemistry

The UV-vis spectroscopy study shown in Figure 3.2 was performed using a UV-vis spectrometer equipped with temperature control set to 298 K. The measurements were performed in a quartz cuvette, containing 3 mL of solution in CH_3CN or water. The stirred sample was degassed by nitrogen, irradiated perpendicularly to the axis of the spectrometer by the beam of a green (λ = 530 nm, $\Delta\lambda_{1/2}$ = 25 nm, 3.02 mW, photon flux 2.1×10^{-8} mol.s^{-1}) or blue (λ = 445 nm, $\Delta\lambda_{1/2}$ = 11 nm, 10.5 mW, photon flux 1.27×10^{-7} mol.s^{-1}) LED fitted to the top of the cuvette, and an absorption spectrum was measured at regular time intervals and analyzed using Microsoft Excel. Mass spectrometry was performed at the beginning and at the end of the irradiation to confirm the nature of the reagent and products. The ^{1}H NMR spectroscopy study of Figure SIII.3 was performed using the white light of a LOT 1000 W Xenon Arc lamp mounted with an infrared and a long pass filter.

3.4.4 Green light irradiation in the cell irradiation set-up

The photochemical reactivity of [**2**](PF$_6$)$_2$ was measured in 96-well plates by dissolving it in cell culturing medium (Opti-MEM complete, 31 μM), followed by irradiation using the green light of the irradiation setup used for cell irradiation (520 nm, 38 J.cm^{-2}) to mimic the conditions of the photocytotoxicity assay. Figure SIII.5 shows that the absorbance change at

300 nm for [**2**]$(PF_6)_2$ after 30 minutes irradiation is leveling off as in no further activation occurs after 30 minutes.

3.4.5 Phototoxicity assay

See Appendix I for comprehensive description of the assay.

3.4.6 Tubulin polymerization assay

For investigation of the ability of the drug to inhibit the polymerization of tubulin in its caged ([**2**]$(PF_6)_2$) and uncaged form (**1**), the fluorescence-based Tubulin Polymerization Assay (Cat. # BK011P) from Cytoskeleton, Inc. Prior was used to conduct the assay, a 2 mM stock solutions of paclitaxel and 16.7 mM solutions of the caged drug and the uncaged drug were prepared in DMSO. These drug stock solutions were then diluted to 250 μM with water to provide aqueous solutions of each drug with a constant DMSO content of 1.5% v/v. At this point, 40 μL samples of the caged drug were pipetted into separate black 96-well plates for irradiation with blue or green light independently. The solutions of the caged drug were then irradiated with either a blue LED (LED Engin LZ1-00B200, 450 nm) or a green LED (LED Engin LZ1-10G102-0000, 523 nm) driven with a BK Precision DC power supply 1630. Light power was measured with a Thorlabs PM50 photometer. Specifically, the appropriate power (W) of light were detected through a 0.6 cm-diameter circular well from a 96-well plate. The green light was used at a power density of 21 $mW.cm^{-2}$ (6 mW, 0.28 cm^2 well). The samples were irradiated for a total of 30 minutes in 10-minute intervals for a total laser exposure of 38 $J.cm^{-2}$. The absorption spectrum of the drug solutions were collected before and after each 10 minutes of irradiation.

For the assay, the following reagents were used. Buffer A contained 80 mM piperazine-N,N′-bis[2-ethanesulfonic acid] sequisodium salt, 2 mM $MgCl_2$, 0.5 mM ethylene glycol-bis(B-amino-ethyl ether)-N,N,N′,N′-tetraacetic acid pH 6.9, and 10 μM fluorescent reporter. Tubulin glycerol buffer contains 80 mM piperazine-N,N′-bis[2-ethanesulfonic acid] sequisodium salt, 2 mM $MgCl_2$, 0.5 mM ethylene glycol-bis(B-amino-ethyl ether)-N,N,N′,N′-tetraacetic acid pH 6.9, and 60% v/v glycerol. Guanosine triphosphate (GTP) stock contains 100 mM. Finally, a tubulin protein stock solution at 10 mg/mL was prepared in a 0.001% v/v solution of GTP in buffer A.

The tubulin reaction mixture used in the assay was prepared by combining 243 μL of buffer A, 112 tubulin glycerol buffer, 4.4 μL of GTP stock, and 85 μL of tubulin stock. This reaction mixture was kept on ice until used within 30 minutes of preparation. A Biotek Synergy H4 hybrid multi-mode plate reader was pre-heated to 37 °C. Prior to starting the assay, a half-area black 96-well plate was preheated within the plate reader. A volume of 5 μL of each of the samples was pipetted into separate wells of the plate and incubated in the warm plate reader for 1 minute. A volume of 45 μL of the tubulin reaction mixture was then mixed into

each of the wells, thereby diluting the drug solutions to the final concentration of 25 μM (total DMSO content of 0.15%). The fluorescence of the samples (λ_{irr} = 360/20 nm, λ_{em} = 485/20 nm) was then recorded every minute for 60 minutes. Paclitaxel at a final concentration of 3 μM was used as a tubulin polymerization inducing control.

3.5 References

1. M. A. Jordan and L. Wilson, *Nat. Rev. Cancer*, 2004, **4**, 253-265.
2. E. K. Rowinsky and R. C. Donehower, *N. Engl. J. Med.*, 1995, **332**, 1004-1014.
3. A.-L. Salmela and M. J. Kallio, *Chromosoma*, 2013, **122**, 431-449.
4. M. Markman, *Supp. Care Cancer*, 2003, **11**, 144-147.
5. D. C. Medellin, Q. Zhou, R. Scott, R. M. Hill, S. K. Frail, R. Dasari, S. J. Ontiveros, S. C. Pelly, W. A. L. van Otterlo, T. Betancourt, C. B. Shuster, E. Hamel, R. Bai, D. V. LaBarbera, S. Rogelj, L. V. Frolova and A. Kornienko, *J. Med. Chem.*, 2016, **59**, 480-485.
6. L. V. Frolova, I. V. Magedov, A. E. Romero, M. Karki, I. Otero, K. Hayden, N. M. Evdokimov, L. M. Y. Banuls, S. K. Rastogi, W. R. Smith, S.-L. Lu, R. Kiss, C. B. Shuster, E. Hamel, T. Betancourt, S. Rogelj and A. Kornienko, *J. Med. Chem.*, 2013, **56**, 6886-6900.
7. M. A. Sgambellone, A. David, R. N. Garner, K. R. Dunbar and C. Turro, *J. Am. Chem. Soc.*, 2013, **135**, 11274-11282.
8. R. N. Garner, J. C. Gallucci, K. R. Dunbar and C. Turro, *Inorg. Chem.*, 2011, **50**, 9213-9215.
9. H. Chan, J. B. Ghrayche, J. Wei and A. K. Renfrew, *Eur. J. Inorg. Chem.*, 2017, **2017**, 1679-1686.
10. N. Karaoun and A. K. Renfrew, *Chem. Commun.*, 2015, **51**, 14038-14041.
11. L. Zayat, C. Calero, P. Albores, L. Baraldo and R. Etchenique, *J. Am. Chem. Soc.*, 2003, **125**, 882-883.
12. Z. Chen, Y. Xiong, R. Etchenique and S. Wu, *Chem. Commun.*, 2016, **52**, 13959-13962.
13. C. Mari, V. Pierroz, S. Ferrari and G. Gasser, *Chem. Sci.*, 2015, **6**, 2660-2686.
14. M. Huisman, J. K. White, V. G. Lewalski, I. Podgorski, C. Turro and J. J. Kodanko, *Chem. Commun.*, 2016, **52**, 12590-12593.
15. K. Arora, J. K. White, R. Sharma, S. Mazumder, P. D. Martin, H. B. Schlegel, C. Turro and J. J. Kodanko, *Inorg. Chem.*, 2016, **55**, 6968-6979.
16. O. Filevich and R. Etchenique, *Photochem. Photobiol. Sci.*, 2013, **12**, 1565-1570.
17. V. H. S. van Rixel, B. Siewert, S. L. Hopkins, S. H. C. Askes, A. Busemann, M. A. Siegler and S. Bonnet, *Chem. Sci.*, 2016, **7**, 4922-4929.
18. L. N. Lameijer, S. L. Hopkins, T. G. Brevé, S. H. C. Askes and S. Bonnet, *Chem. Eur. J.*, 2016, **22**, 18484-18491.
19. B. Siewert, V. H. S. van Rixel, E. J. van Rooden, S. L. Hopkins, M. J. B. Moester, F. Ariese, M. A. Siegler and S. Bonnet, *Chem. Eur. J.*, 2016, **22**, 10960-10968.
20. R. E. Goldbach, I. Rodriguez-Garcia, J. H. van Lenthe, M. A. Siegler and S. Bonnet, *Chem. Eur. J.*, 2011, **17**, 9924-9929.
21. V. H. S. van Rixel, A. Busemann, A. J. Göttle and S. Bonnet, *J. Inorg. Biochem.*, 2015, **150**, 174-181.
22. S. L. Hopkins, B. Siewert, S. H. C. Askes, P. Veldhuizen, R. Zwier, M. Heger and S. Bonnet, *Photochem. Photobiol. Sci.*, 2016, **15**, 644-653.
23. T. J. McMillan, E. Leatherman, A. Ridley, J. Shorrocks, S. E. Tobi and J. R. Whiteside, *J. Pharm. Pharmacol.*, 2008, **60**, 969-976.
24. S. Wäldchen, J. Lehmann, T. Klein, S. van de Linde and M. Sauer, *Sci. Rep.*, 2015, **5**, 15348.
25. S. Prasad, S. C. Gupta and B. B. Aggarwal, *Trends Pharmacol. Sci.*, 2016, **37**, 435-450.
26. K. S. Chan, C. G. Koh and H. Y. Li, *Cell Death and Dis.*, 2012, **3**, e411.
27. J. Broichhagen, J. A. Frank and D. Trauner, *Acc. Chem. Res.*, 2015, **48**, 1947-1960.
28. W. A. Velema, W. Szymanski and B. L. Feringa, *J. Am. Chem. Soc.*, 2014, **136**, 2178-2191.
29. M. Dong, A. Babalhavaeji, S. Samanta, A. A. Beharry and G. A. Woolley, *Acc. Chem. Res.*, 2015, **48**, 2662-2670.
30. M. Schönberger and D. Trauner, *Angew. Chem., Int. Ed.*, 2014, **53**, 3264-3267.
31. S. Samanta, C. Qin, A. J. Lough and G. A. Woolley, *Angew. Chem., Int. Ed.*, 2012, **51**, 6452-6455.
32. S. Samanta, T. M. McCormick, S. K. Schmidt, D. S. Seferos and G. A. Woolley, *Chem. Commun.*, 2013, **49**, 10314-10316.
33. M. M. Lerch, M. J. Hansen, W. A. Velema, W. Szymanski and B. L. Feringa, *Nat. Comm.*, 2016, **7**, 12054.

34. S. Bonnet, *Comments Inorg. Chem.*, 2015, **35**, 179-213.
35. D. Crespy, K. Landfester, U. S. Schubert and A. Schiller, *Chem. Commun.*, 2010, **46**, 6651-6662.
36. J. D. Knoll, B. A. Albani and C. Turro, *Acc. Chem. Res.*, 2015, **48**, 2280-2287.
37. N. J. Farrer, L. Salassa and P. J. Sadler, *Dalton Trans.*, 2009, **48**, 10690-10701.